1987

An investigation of unipolar arcing at atmospheric pressure in Aluminum 2024 and aluminum coated glass slides.

Woodson, Steven Wayne.

NAVAL POSTGRADUATE SCHOOL
Monterey, California

THESIS

AN INVESTIGATION OF UNIPOLAR ARCING AT ATMOSPHERIC PRESSURE IN ALUMINUM 2024 AND ALUMINUM COATED GLASS SLIDES

by

Steven Wayne Woodson

June 1987

Thesis Advisor: F. R. Schwirzke

Approved for public release; distribution is unlimited.

SECURITY CLASSIFICATION OF THIS PAGE

REPORT DOCUMENTATION PAGE

1a REPORT SECURITY CLASSIFICATION UNCLASSIFIED	1b RESTRICTIVE MARKINGS
2a SECURITY CLASSIFICATION AUTHORITY	3 DISTRIBUTION/AVAILABILITY OF REPORT Approved for public release; distribution is unlimited.
2b DECLASSIFICATION/DOWNGRADING SCHEDULE	
4 PERFORMING ORGANIZATION REPORT NUMBER(S)	5 MONITORING ORGANIZATION REPORT NUMBER(S)
6a NAME OF PERFORMING ORGANIZATION Naval Postgraduate School 6b OFFICE SYMBOL (If applicable) 61	7a NAME OF MONITORING ORGANIZATION Naval Postgraduate School
6c ADDRESS (City, State, and ZIP Code) Monterey, California 93943-5000	7b ADDRESS (City, State, and ZIP Code) Monterey, California 93943-5000
8a NAME OF FUNDING/SPONSORING ORGANIZATION 8b OFFICE SYMBOL (If applicable)	9 PROCUREMENT INSTRUMENT IDENTIFICATION NUMBER
8c ADDRESS (City, State, and ZIP Code)	10 SOURCE OF FUNDING NUMBERS PROGRAM ELEMENT NO / PROJECT NO / TASK NO / WORK UNIT ACCESSION NO

11 TITLE (Include Security Classification)
AN INVESTIGATION OF UNIPOLAR ARCING AT ATMOSPHERIC PRESSURE IN ALUMINUM 2024 AND ALUMINUM COATED GLASS SLIDES

12 PERSONAL AUTHOR(S)
Woodson, Steven W.

13a TYPE OF REPORT	13b TIME COVERED	14 DATE OF REPORT (Year, Month, Day)	15 PAGE COUNT
Master's Thesis	FROM _____ TO _____	June 1987	53

16 SUPPLEMENTARY NOTATION

17 COSATI CODES			18 SUBJECT TERMS (Continue on reverse if necessary and identify by block number)
FIELD	GROUP	SUB-GROUP	Unipolar, Unipolar Arcing

19 ABSTRACT (Continue on reverse if necessary and identify by block number)

An experimental investigation of unipolar arcing at atmospheric pressure was conducted using Aluminum 2024 and glass slides with a thin coating of pure aluminum. The plasma was produced on the surface using a neodymium-glass laser in the Q-switched mode. It was found that the power density required for the onset of unipolar arcing was similar to that of samples irradiated in a vacuum, although the size and density of the resulting craters were significantly different.

20 DISTRIBUTION/AVAILABILITY OF ABSTRACT ☒ UNCLASSIFIED/UNLIMITED ☐ SAME AS RPT ☐ DTIC USERS	21 ABSTRACT SECURITY CLASSIFICATION UNCLASSIFIED
22a NAME OF RESPONSIBLE INDIVIDUAL F. R. Schwirzke	22b TELEPHONE (Include Area Code) 646-2635 22c OFFICE SYMBOL 61Sw

DD FORM 1473, 84 MAR 83 APR edition may be used until exhausted
All other editions are obsolete

SECURITY CLASSIFICATION OF THIS PAGE
UNCLASSIFIED

Approved for public release; distribution is unlimited.

An Investigation of Unipolar Arcing at Atmospheric Pressure in Aluminum 2024 and Aluminum Coated Glass Slides

by

Steven Wayne Woodson
Lieutenant, United States Navy
B.O.E., University of Mississippi, 1979

Submitted in partial fulfillment of the requirements for the degree of

MASTER OF SCIENCE IN PHYSICS

from the

NAVAL POSTGRADUATE SCHOOL
June 1987

ABSTRACT

An experimental investigation of unipolar arcing at atmospheric pressure was conducted using Aluminum 2024 and glass slides with a thin coating of pure aluminum. The plasma was produced on the surface using a neodymium-glass laser in the Q-switched mode. It was found that the power density required for the onset of unipolar arcing was similar to that of samples irradiated in a vacuum, although the size and density of the resulting craters were significantly different.

TABLE OF CONTENTS

I. INTRODUCTION

One of the most active areas of research that the scientific community is currently engaged in is that of power production. Fusion energy sources in particular have received great emphasis. In most fusion reactor design studies, the plasma is confined by strong magnetic fields. Some of the plasma will, however, diffuse perpendicular to the field lines and come into contact with the surrounding walls. This has led to extensive studies involving the interaction of a hot dense plasma with a surface. These studies have revealed that erosion due to several processes occurs. These processes include sputtering, unipolar arcing, pulse heating, and gas implantation [Ref. 1].

The process involved in sputtering is a momentum transfer process. When an energetic neutral atom or ion hits the solid surface it imparts its energy to a surface atom, and if this energy exceeds its binding energy, the particle can be released into the plasma [Ref. 2]. Heat pulses are a result of nonuniform energy deposition onto the wall from the plasma and may lead to localized evaporation and surface cracking. Gas implantation results when high energy hydrogen or helium plasma ions impact on the first wall. The ones that are not directly backscattered come to rest in the wall, generally at

an interstitial site [Ref. 1]. Unipolar arcing is a process where an arc is established between the wall and the plasma with the wall acting as both the anode and cathode.

These erosion processes lead to two major areas of concern. The first is that various components of the reactor will be damaged, resulting in a limited lifetime. The second, and perhaps more significant, is that these erosion processes introduce impurities into the plasma, and these impurities limit the available plasma parameters [Ref. 1: p. 1047]. In an article by T. Taxima, he states that "the major energy losses from the present day's tokamak plasmas are those to impurities" [Ref. 3].

Evidence of unipolar arcing (i.e. arc tracks) has been observed in DITE, as well as PLT, ISX, Macrator and Pulsator Tokamaks [Ref. 4]. The arc tracks appear on the fixed limiter, probes inserted in the plasma and on parts of the torus vacuum structure. A study on impurity levels and erosion rates showed that unipolar arcing is the dominant mechanism for impurity production [Ref. 5]. This is due to the fact that unipolar arcing is not a homogeneous energy deposition process, but rather one whereby the energy from the plasma is concentrated towards the cathode spots [Ref. 6].

Plasma surface interactions are also important in newly evolving areas of technology. For example, weapon system

designs for both high energy lasers and particle beams include high speed plasma switches. The contacts on the switches will operate in a plasma environment and will be subject to these erosion processes. Also, in high energy laser weapons a plasma could be formed at the target which will result in surface damage. It is not known how severe this plasma surface damage will be compared to other damage mechanisms, but conceivably it could be significant.

Although unipolar arcing was first observed in the late 1950's, other problems dominated the fusion program and interest in arcing diminished. It was not until the late 1970's that interest in unipolar arcing was revived, and since that time it has been an area receiving much study, although the process is still not fully understood. For this thesis, experimentation was done to observe plasma-surface damage which occurs at atmospheric pressure on a good conducting material (type 2024 Aluminum) and on a poor conductor (a glass slide) that was coated with a thin film of aluminum.

The specific goals of this thesis were twofold. The first was to conduct a systematic experimental study to observe unipolar arcing at atmospheric pressure, determine the power density required for the onset of arcing (on type 2024 Aluminum targets) and compare the observed results to those previously reported. Secondly, it was a goal to try to

photograph the arcing events as they were occurring. For this, the aluminum coated glass slides were used with a camera placed behind the targets.

The following section deals with the theory of the unipolar arcing phenomenon and gives details of the underlying model on unipolar arcing.

II. BACKGROUND AND THEORY OF UNIPOLAR ARCING MODELS

A. ROBSON-THONEMANN MODEL

In 1958 Robson and Thonemann proposed the first model of an arcing phenomenon which "requires only one electrode and is maintained by the thermal energy of the plasma electrons" [Ref. 7]. They called this phenomenon "unipolar arcing." Two experiments were also conducted which verified their theory. In these, a strong plasma was generated by an electrodeless high-frequency discharge in a mercury cathode tube which was evacuated to a gas pressure of less than 10^{-6} mm Hg. An arc was then established by an externally applied anode voltage. As the plasma density increased, the arc current increased. The externally applied voltage was then turned off, but the arc continued to burn in the unipolar mode until the plasma density became too low to sustain it.

The basis of their theory lies in the idea that a floating potential is established between a plasma and the exposed metal plate. Within a plasma, the ion temperature (T_i) does not necessarily equal the electron temperature (T_e). The electrons will have a much higher thermal velocity than will the ions due to their relatively small mass. When in the vicinity of a wall, many more electrons will initially contact the wall, resulting in a negative potential relative to the plasma. (One of the defining conditions for the

existence of a plasma is that it is "a quasineutral gas of charged and neutral particles" [Ref. 8]. The idea behind quasineutrality is that if the plasma dimensions are large compared to a characteristic length called the Debye Length, then it will shield itself from electric potentials (or electric fields) in a distance on the order of the Debye Length. This results in the formation of a potential sheath (Fig. 2.1) which prevents all but the most energetic of the electrons to reach the wall while at the same time it functions to accelerate the ions within the sheath. The plasma potential will build up to the point where the ion loss level is equal to the electron loss level, thus maintaining an equilibrium situation where the net current is zero. For singly charged ions the sheath potential is given by:

$$V_f = \frac{kT_e}{2e} \ln \frac{M_i}{2\pi M_e} \qquad \text{(Eqn. 2.1)}$$

where

k = Boltzmann Constant

e = charge of the electron

T_e = electron temperature

M_e = electron mass

M_i = ion mass

If the value of this floating potential exceeds a certain value, an arc will be initiated and sustained on the isolated plate. If a cathode spot is initiated on the plate, there will be a strong local emission of electrons from it. This results in a reduction in the floating potential to the value of V_c. More electrons can then reach the plate, closing the current loop and maintaining the plasma's quasineutrality. This circulating current is given by [Ref. 9]:

$$I_c = An_e\left[\frac{kT_e}{2\pi M_e}\right]^{\frac{1}{2}}\left[\exp\frac{(-eV_c)}{(kT_e)} - \exp\frac{(-eV_f)}{(kT_e)}\right] \qquad \text{(Eqn 2.2)}$$

where

n_e = electron plasma density

A = area of the exposed plate

In order to maintain a stable cathode spot, there is a lower limit for I_c. Above this value the arc will be maintained, and below it, it will not. This critical value of current is dependent on the material of the plate and is on the order of 10 Amperes.

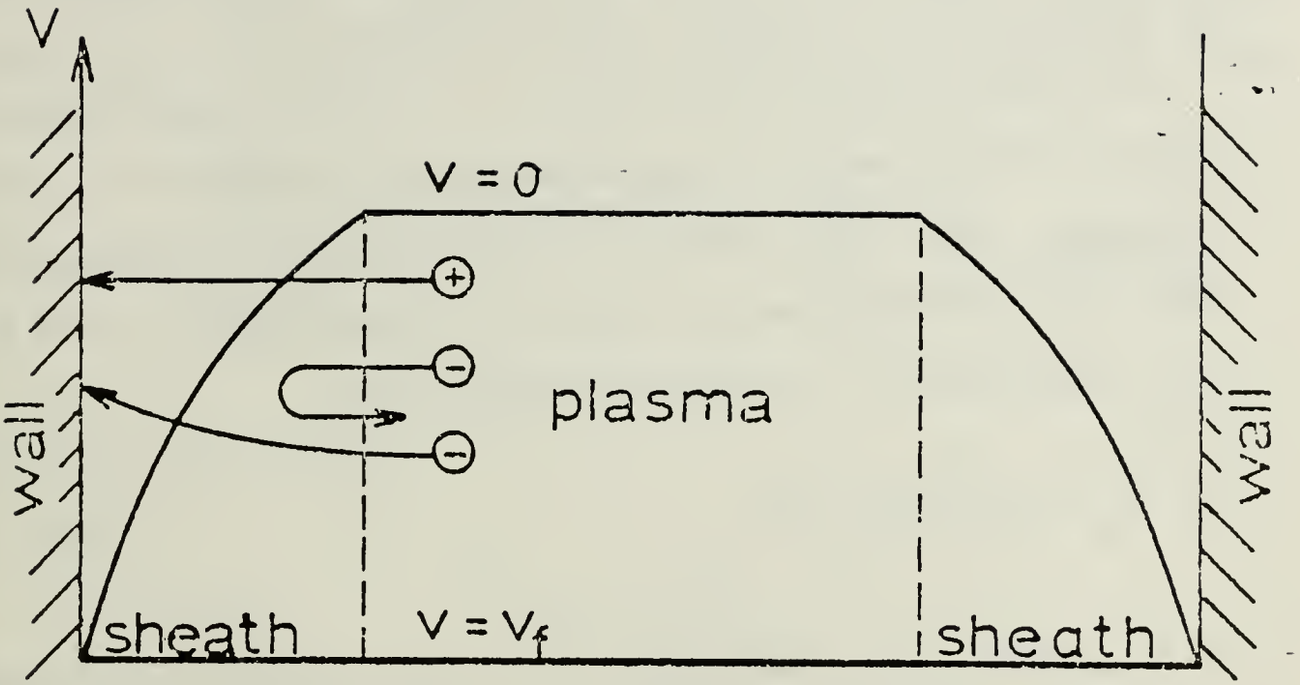

Figure 2.1 Plasma-Wall Potential Sheath.

This model is widely referenced in many papers dealing with unipolar arcing and is generally accepted to explain the basic process of unipolar arcing. However, this model does not address many of the specifics of what is happening, and in order to gain a better understanding of this phenomenon, a more detailed model must be examined.

B. TAYLOR-SCHWIRZKE MODEL

An expanded version of the unipolar arcing phenomenon was introduced in 1980 by Schwirzke and Taylor [Ref. 10]. This

model expands on the basic ideas presented in the Thonemann model by elaborating "upon the electric fields which are set up in the plasma and drive the arc" [Ref. 11].

As discussed previously, a sheath potential is established between the plasma and the surface (as given by Equation 2.1). The length (perpendicular to the surface) over which this potential exists is proportional to the Debye Shielding Length (λ_d) which is given by:

$$\lambda_d = (kT_e/4\pi n_e^2)^{\frac{1}{2}} \qquad \text{(Eqn. 2.3)}$$

In order for an arc to develop, V_f must increase sufficiently for an arc to ignite and be sustained. Another necessry condition, they argue, is that the density of ions above the cathode spot increases in order for a larger electron current to flow from the surface into the plasma (this is different from the previously discussed model in that it implies a constant plasma density). This increase is due to the ionization of neutral particles being released from the cathode spot (Fig. 2.2). Cathode spots can initiate from surface protrusions, inclusions, micro-whiskers, or other metallurgical inhomogeneities.

This idea (of where the cathode spot begins) is consistent with a study done by Tien, Panayotou, Stevenson, and Gross on different materials which had been prepared

similarly, but upon which some samples were slightly etched to expose their characteristic grain structure. They found that the etched samples had evidence of a higher area

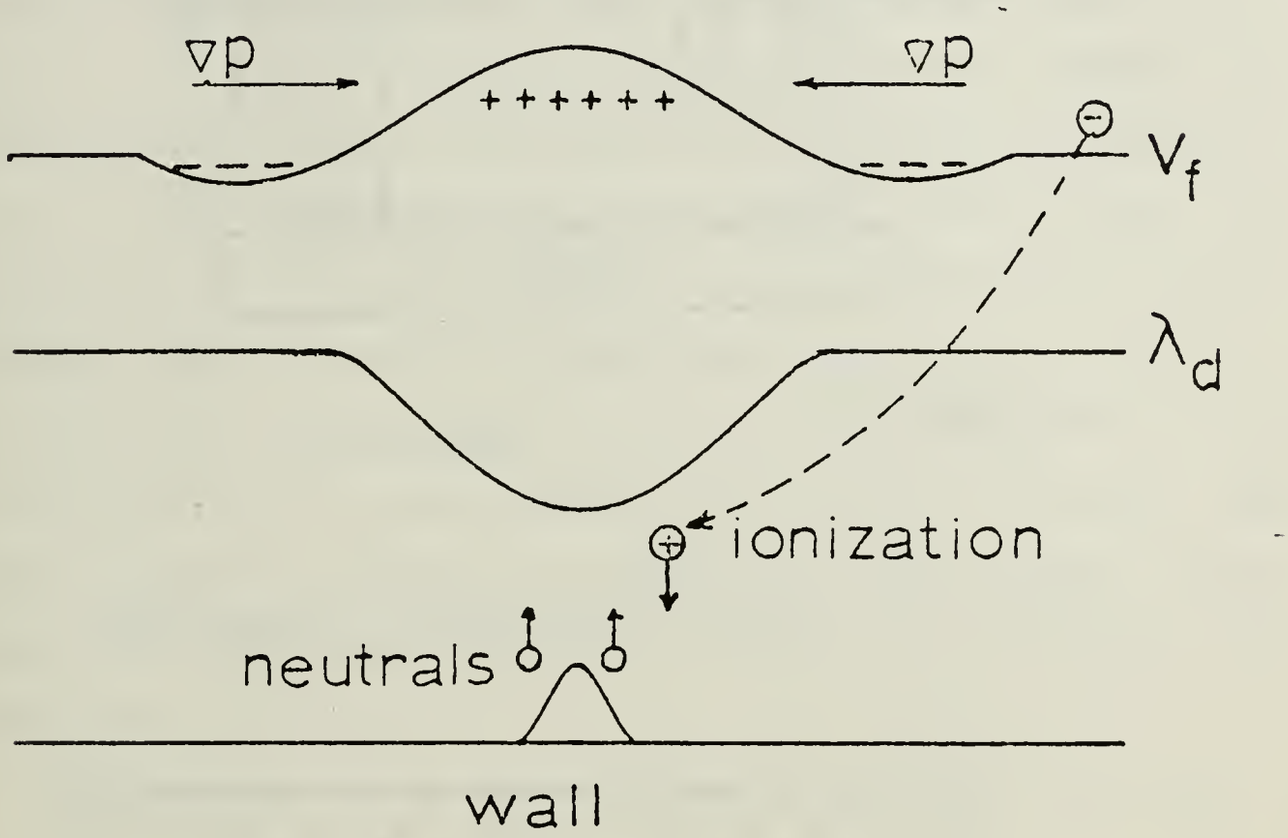

Figure 2.2 Schwirzke-Taylor Unipolar Arc Model.

coverage of arcing than did the polished samples. They also reported that "the locations of the arc spots are not random in the slightly etched samples." They continue by saying, "It is interesting that, on the polished specimens, ..., arc spots are more randomly distributed." One of their main conclusions is that the cathode spots are preferentially initiated at microstructural inhomogeneities [Ref. 12]. Figures 2.3 and 2.4 illustrate this.

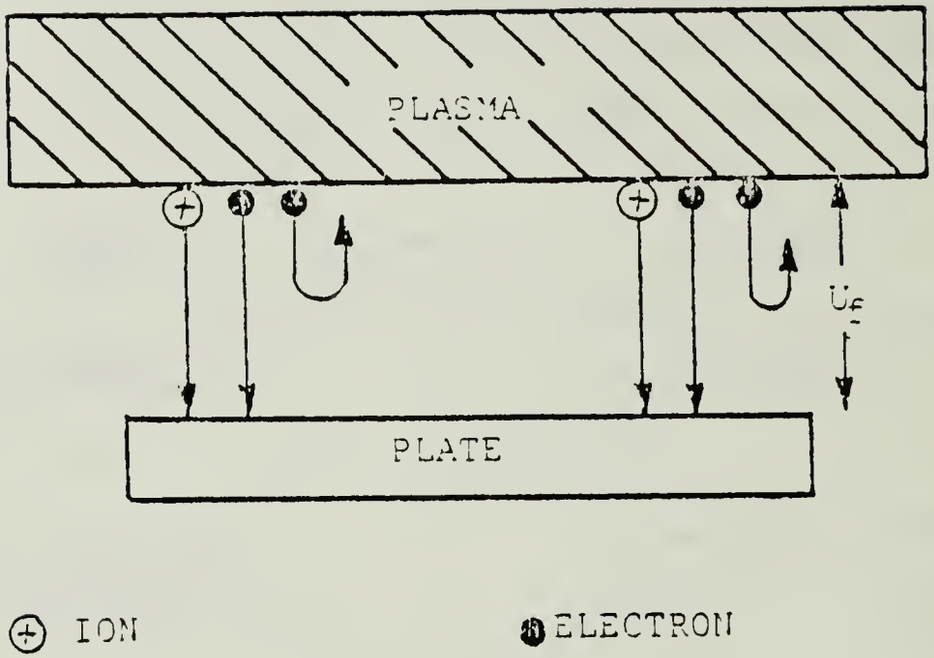

Figure 2.3 Isolated Plate Without Cathode Spot.

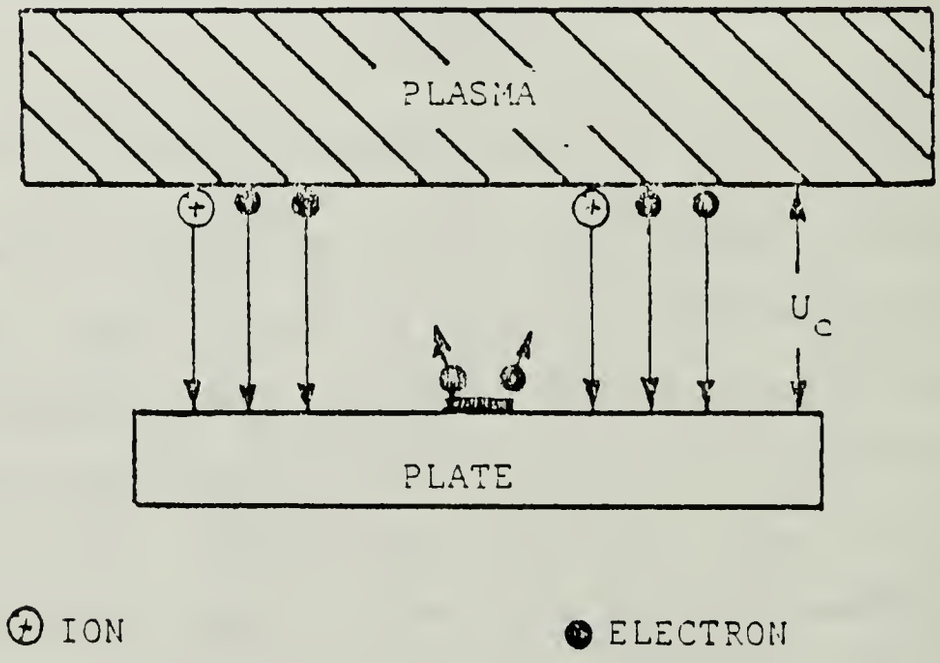

Figure 2.4 Isolated Plate with Cathode Spot.

Using values which are characteristic of tokamak edge plasmas, Schwirzke and Taylor calculate the Debye Length (λ_d) to be on the order of 10^{-3} cm. Making assumptions about the neutral particle density (n_d) in the sheath (which is a function of the desorption and evaporation rates) and assuming a value for the ionization cross section, the mean free path length can be calculated. From this, the probability for ionization of a neutral particle can be found. Using the assumed plasma and surface characteristics, a probability of 2×10^{-2} was calculated. This leads to an increase in the plasma density by a factor of 4000. The Debye Length is inversely proportional to the square root of the electron plasma density, and decreases by a factor of about 60.

The electric field in the normal direction is given by:

$$E_n \simeq V_f/\lambda_d \qquad \text{(Eqn 2.4)}$$

Therefore a decrease in the Debye Length will cause a corresponding increase in the electric field which accelerates the ions towards the surface. The increased number of ions bombarding the surface leads to an increase in surface temperature which causes more desorption and evaporation, and the process continues.

The increase of the plasma density above the cathode spot also leads to a radial electrical field given by:

$$E_r = \frac{-kT_e}{en_e} \frac{dn_e}{dr} \qquad \text{(Eqn 2.5)}$$

This causes a lowered potential in a ring-like area which allows electrons to return to the surface and maintain the plasma's quasineutrality. The lowered potential (ΔV) is:

$$\Delta V = \frac{kT_e}{e} \ln \frac{n_e}{n_{eo}} \qquad \text{(Eqn 2.6)}$$

Equating the sheath potential to ΔV yields:

$$\frac{kT_e}{2e} \ln \frac{M_i}{2\pi M_e} = \frac{kT_e}{e} \ln \frac{n_e}{n_{eo}} \qquad \text{(Eqn 2.7)}$$

With zero sheath potential, the electron saturation current to a surface over A is:

$$I_s = \frac{en_e \bar{V}_e A}{4} \qquad \text{(Eqn 2.8)}$$

Solving for area (A) and using commonly occurring values for the variables in the equation, a radius on the order of 10 microns is obtained. This value for the return current area is of the same order as the radius of the outer crater rim,

suggesting that the location of the outer crater rim is an indication of how far the return current area has expanded during the burn time of the arc.

The Robson and Thonemann model stated that the area was the whole surface area that was exposed to the plasma. It was once thought that if the exposed surface was subdivided by insulating strips, arcing would be prevented, however, for areas of the magnitude predicted from the Schwirzke and Taylor model, this is clearly impractical.

While the Robson and Thonemann model seems to account for the basic mechanism of unipolar arcing, this (Taylor and Schwirzke) model predicts the occurrence of the cathode spot hole which is due to high rates of desorption and evaporation. It also suggests relatively small values for the area of the return current.

III. EXPERIMENTAL DESIGN AND PROCEDURES

A. EXPERIMENTAL DESIGN

Target samples were irradiated by a neodymium glass laser to produce a plasma at the surface. The initial aim of this thesis was to then attempt to photograph the resultant unipolar arcing. Several difficulties, however, arose to prevent this. Primarily there was the problem of obtaining a camera that would satisfactorily accomplish the task. The primary stipulation on the camera was to be able to obtain magnifications on the order of at least 100X. In order to accomplish this, with available equipment, the camera had to be approximately an inch from the target. This immediately precluded the ability to use the evacuated target test chamber, since the viewing port is approximately eight (8) inches from the target. Even when the target was mounted outside the chamber no acceptable manner of positioning the camera could be found that would yield a direct enough picture, be out of the primary laser beam, and where the camera's optics could be protected against the resulting plasma and reflected radiation.

The next approach was to use a thin target (less than 5 micrometers thick since that is the approximate depth of the ensuing crater) and attempt to photograph arcing from behind

the target. In a setup of this manner, an attenuating filter could be placed between the target and the camera which would protect the camera from the laser radiation and there would be virtually no limit to how close the camera could be positioned to the target. With this in mind, a vacuum deposition of aluminum was placed onto glass microscope slides. Two thicknesses of the coatings were used (thin coatings of approximately .2μm and a thick coating of approximately 1 μm).

The process of unipolar arcing in atmospheric pressure has not been studied. A second procedure involving irradiating aluminum targets in atmosphere with a neodymium glass laser was done in order to determine the onset of arcing. All samples were examined under an optical and a scanning microscope to determine the surface conditions before and after the plasma surface interaction. Figure 3.1 is a schematic of the experimental setup.

B. EQUIPMENT

1. Laser

A KORAD K-1500 Q-switched neodymium glass laser was used to irradiate the test samples producing a hot-dense plasma over the surface. The laser outputs a wavelength of 1.06 micrometers. Nominal output energy ranges from .2-15J, depending on the applied voltage to the oscillator and

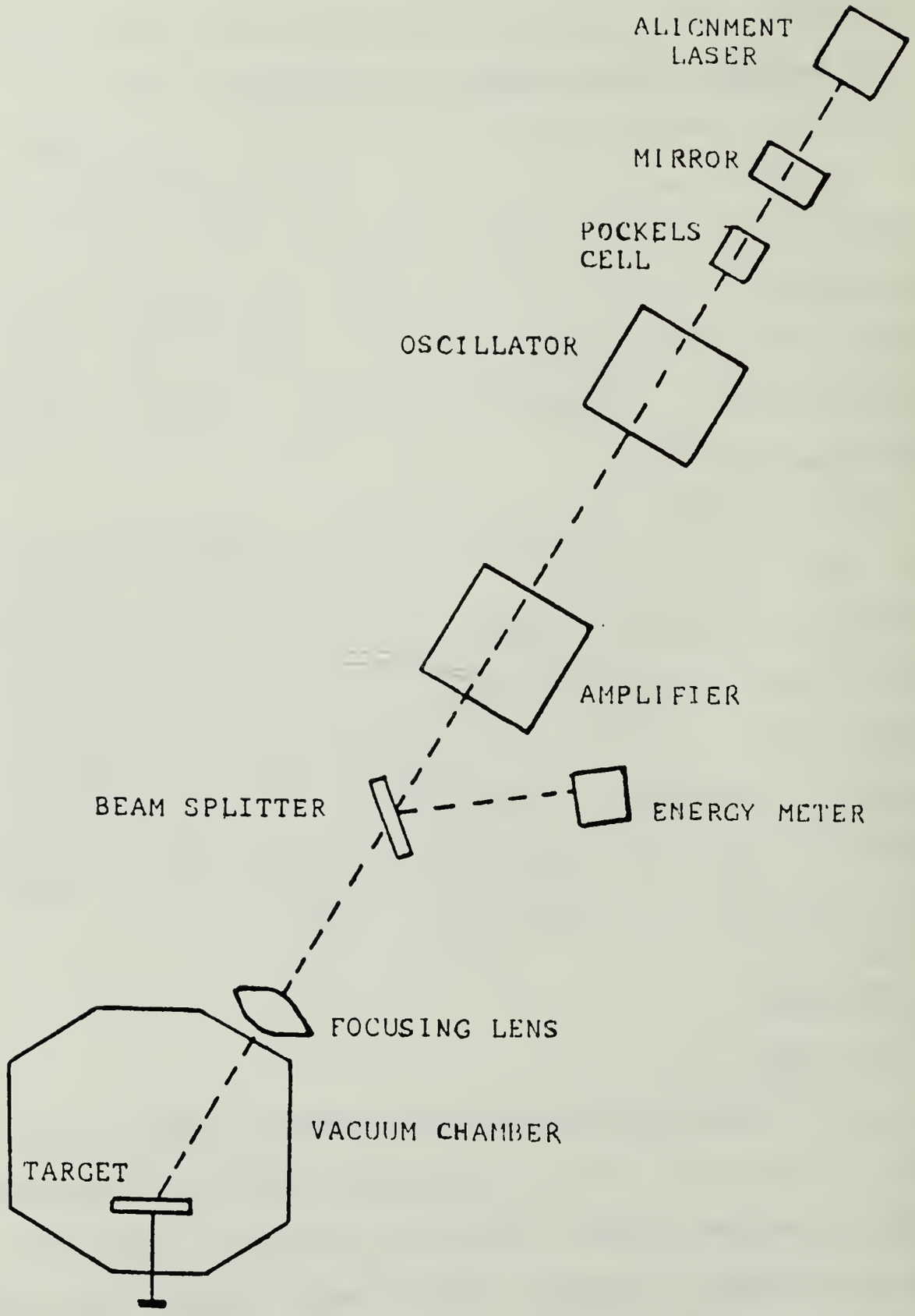

Figure 3.1 Experimental Setup.

amplifier flash lamps. It was found to be easier and more controllable to use constant voltages to the amplifier and oscillator and reduce the energy by placing transmission filters in the path of the beam. The output energy was measured using a Laser Precision RK-3200 Series Pyroelectric Energy Meter calibrated to an accuracy of about 20%. Nominal pulse width is 25 nanoseconds, and the unfocused beam has a cross sectional area of 4.04 $\pm$ .2 cm^2.

2. Optical Microscope

The optical microscope that was used is a Bausch and Lomb stereoscopic light microscope. Magnification ranges from 20X to 800X. The target samples were observed before and after laser illumination.

3. Scanning Electron Microscope

The Scanning Electron Microscope used was a Cambridge Stereoscan S4-10. The images obtained were formed from secondary electrons. It has the capability of magnifications in the range from 20X to 100,000X.

4. Target Test Chamber

The aluminum 2024 target samples were mounted in a cubic target test chamber (maintained at atmospheric pressure) with an internal volume of 12.9 $\pm$ 0.3 liters. The chamber is composed of unbaked aluminum with a target holder probe running into the chamber that can be rotated for alignment and to expose fresh target samples. The targets

are aligned at 30 degrees to the laser beam. A focusing lens was mounted on the chamber to obtain the desirable laser beam spot size.

C. TARGET PREPARATION

1. Aluminum Coated Microscope Slides

The microscope slides used in this portion of the experiment are of an ordinary soda-lime window glass type. The approximate composition is 72% Selica (SiO_2), 15% Soda (Na_2O), 9% Lime (CaO), 3% Magnesium Oxide (MgO), Aluminum Oxide (Al_2O_3) and .03% Iron (Fe_2O_3).

The slides were thoroughly cleaned with soap and water and then with methyl alcohol. They were then coated with a thin film of pure (99.99%) aluminum. The deposition of aluminum on the slide surface was accomplished by an evaporation process under high vacuum using a Veeco Series 401 system. The slides were then stored in a desicator until ready for use, at which point any surface dust was removed by using high pressure freon gas.

The thickness of the aluminum coatings was approximated by comparing the mass of the slide before and after depositing the aluminum coating. This assumes a uniform thickness of aluminum on the coated area.

2. Aluminum Targets

The disk targets were made of type 2024 aluminum. They were machined on a lathe to a final diameter of approximately 1/4 inch. The samples were mounted in bakelite and rough sanded. They were then polished using an AB Duo Belt Wet Sander (400 grit) and fine ground using 600 grit wet paper. Following this, they were dry sanded and polished using three (3) slurries of .05 Al_2O_3 to reduce surface roughness.

The specimens were then removed from the bakelite, cleaned with methyl alcohol and ultrasonically cleaned in acetone. They were then stored in a desicator until ready for use in the target chamber.

IV. EXPERIMENTAL RESULTS

A. TYPE 2024 ALUMINUM TARGETS

1. Description

Numerous highly polished Aluminum 2024 targets were irradiated in the target chamber at atmospheric pressure. The power density was varied by the use of transmission filters and the energy was measured with the energy meter. The beam spot size was controlled by using a glass lens and was measured by irradiating an exposed Polaroid film at the target plane and then measuring the diameter of the spot. Using an oscilloscope, the 3 db pulse width was found to be 20 nanoseconds. A hand held Polaroid camera was positioned above the targets to note any plasma formation.

2. Target Damage

After being exposed to the laser radiation each sample was observed using an optical and scanning electron microscope. Target damage was in the form of unipolar arcing and surface melting. Figure 4.1 shows target damage in the region of maximum irradiation. In all of the field of view with the exception of the right central portion it is evident that melting has occurred. At greater magnification, Figure 4.2 shows the boundary region of melting. The plasma flow direction away from the focal spot in the figure is from top

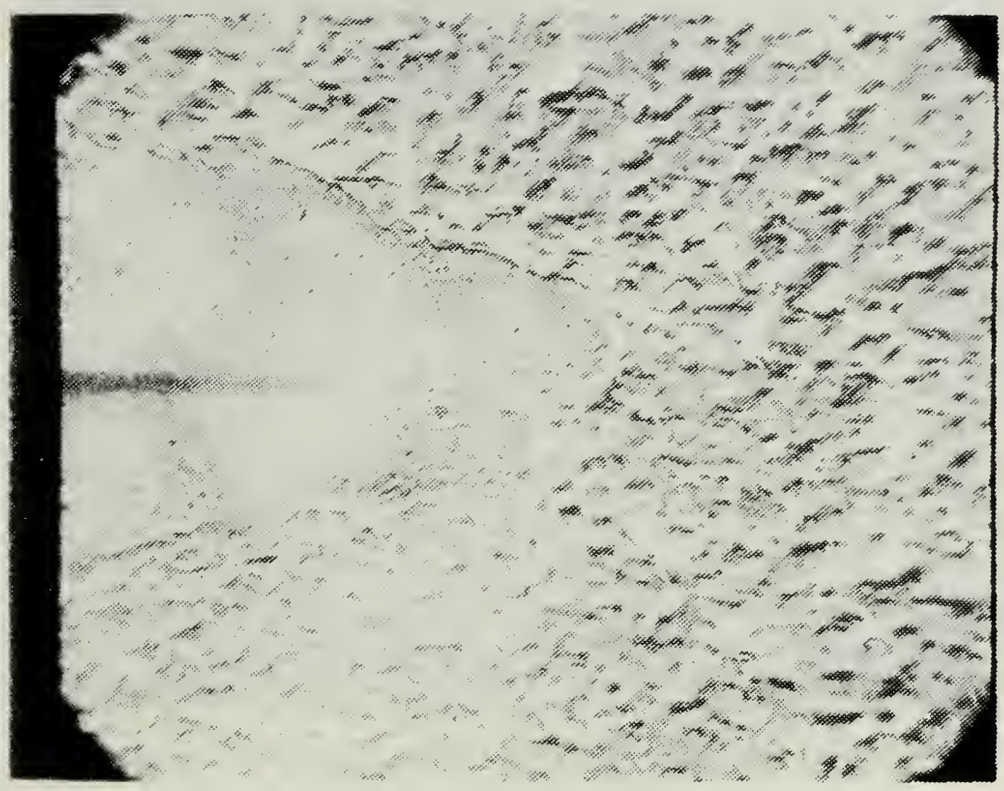

Figure 4.1 High Irradiance Region of Aluminum Target, 220X, SEM

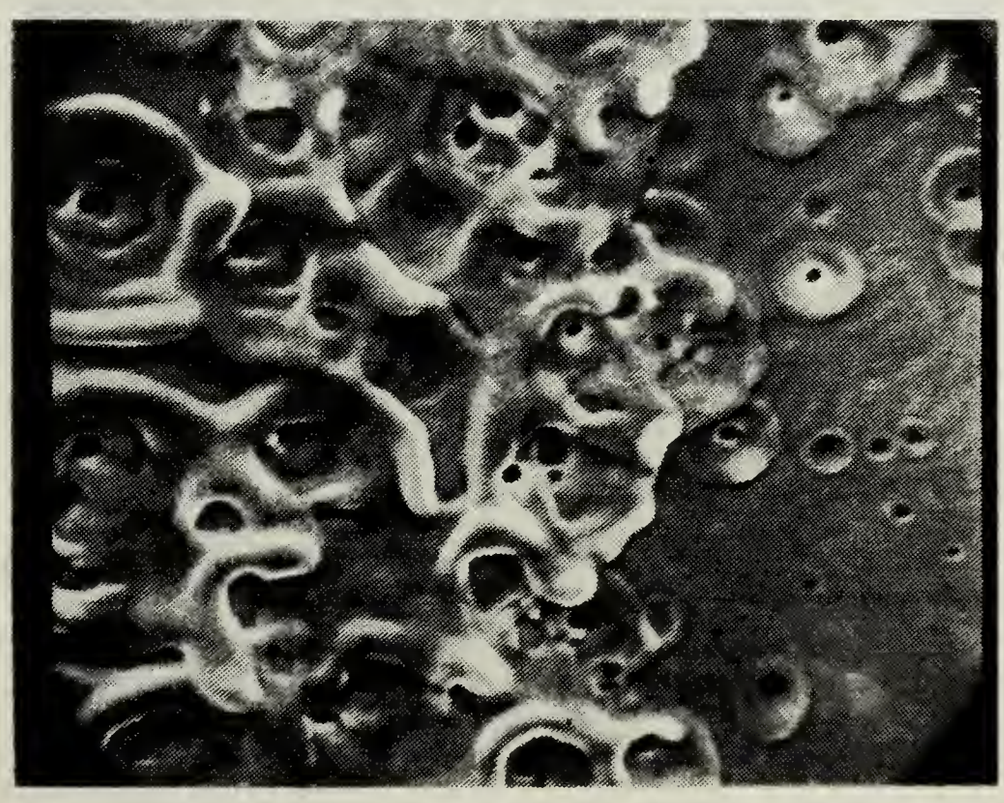

Figure 4.2 Boundary Region for Melting on Aluminum Target, 1200X, SEM

to bottom. The small holes around which the flow was diverted are the craters where, simultaneously, unipolar arcing was occurring. Outside of the region of the melting, unipolar arcing was the only visible damage mechanism as evidenced by the characteristic crater and rim formation.

At lower energy densities the only observable damage mechanism was unipolar arcing. Figure 4.3, at 220X magnification, using the scanning electron microscope, shows the region of maximum intensity on a sample irradiated at an order of magnitude less energy density than the preceding figures where melting was evident. The unipolar arc craters are not evenly distributed, but are bunched in locally concentrated areas. This is partially due to hot spots in the laser beam but also may be a result of surface inhomogeneities where arcing is initiated (such as surface inhomogeneities like whiskers or at grain boundaries). At high magnification, Figure 4.4 clearly shows the unipolar arc craters. The crater density is on the order of 1.7×10^6 craters per square centimeter.

Further analysis from Figure 4.5 at higher magnification shows a distinctive view of the unipolar arc craters. The craters with the largest diameter, 12 to 13 microns, correspond to a long arc duration as compared to the ones with small diameters, 3 to 4 microns. The central dark regions are the cathode spots and range from .08 microns to

Figure 4.3 Unipolar Arcing on the Aluminum Target, 220X, SEM

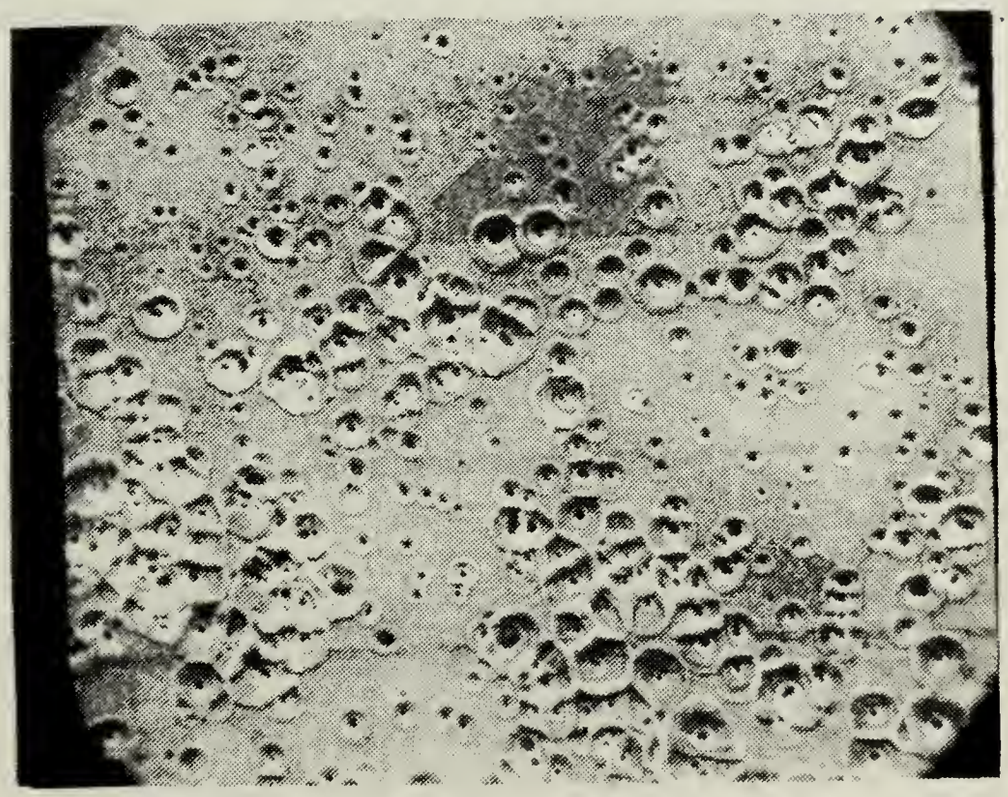

Figure 4.4 Unipolar Arc Craters on Aluminum Target, 540X, SEM

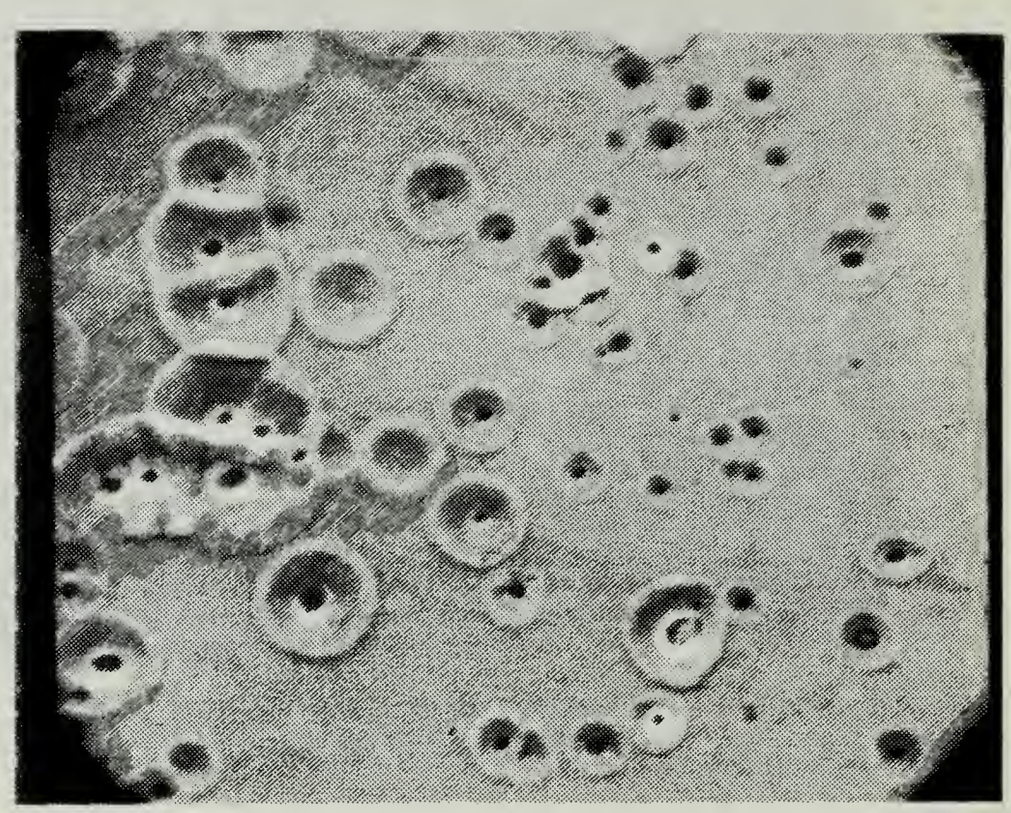

Figure 4.5 Unipolar Arc Craters on Aluminum Target, 1200X, SEM

2.5 microns in diameter, again a function of the arc duration time. The hemispherical crater is formed by the outflow of molten metal where localized melting has occurred due to the radial plasma pressure.

3. Determination of Power Density Required for the Onset of Unipolar Arcing

a. Experimental Results

The incident energy upon various Aluminum 2024 targets was systematically varied in order to determine the

minimum power density required for unipolar arcing to occur. Average power density, $\bar{F}$, can be calculated by:

$$\bar{F} = \bar{E}/AT$$

where E = Incident Energy

A = Exposed Area

T = 3 db pulse width

A summary of results is contained in Table I.

b. Analysis of Results

From these results an indication of the onset of arcing can be determined although there are some inconsistencies in the data. Targets 1a and 2 showed no evidence of arcing while targets 8 and 12 had arcing damage even though the calculated value for power density was lower. It is important to note that targets 1a through 5 were irradiated on the same day and that targets 6 through 13 were irradiated approximately three days later.

From the first group (1a through 5) it can be stated that the onset of arcing occurs between 13.1 and 20.3 MW/cm^2. The second group (6 through 13) indicates a region of between 6.8 and 9.7 MW/cm^2. Although these values differ, the data obtained in each group is self consistent.

There are at least three possible explanations for the inconsistencies in the data. These are:

TABLE I. SUMMARY OF RESULTS TO DETERMINE THE ONSET OF ARCING FOR ALUMINUM 2024 AT ATMOSPHERIC PRESSURE

Target	Calculated Power Density (MW/CM^2)	Light	Arcing
1a	13.1	no	no
1b	103.0	yes	yes
2	12.6	no	no
3	26.4	yes	yes
4	20.3	yes	yes
5	19.4	no	no
6	31.7	yes	yes
7	21.2	yes	yes
8	9.7	no	yes
9	101.0	yes	yes
10	17.6	no	yes
11	29.0	yes	yes
12	10.6	no	yes
13	6.8	no	no

(1) The targets were somehow different (due to formation of aluminum oxide with time).

(2) The diagnostic instrumentation was different.

(3) The laser mode was different.

Any one of the above or a combination of the above could have caused the results to differ from one another.

All of the above targets were identically prepared and stored in a desicator until their use. It is conceivable, however, that between the time the first and second groups were irradiated the surface of the targets changed due to absorption of moisture or to surface oxidation or contamination. A change in the surface characteristics could have caused a different point for the onset of arcing.

The hardware and experimental setup on the two days in question was identical. It was noted, however, that the energy meter had regions of deterioration on the detector surface. Although care was taken on both days to avoid those regions, it is possible that alignment on one of the days was such that enough energy was incident on those regions to account for the change in indicated energy.

The next possible cause is the output mode of the laser. As previously stated, the intensity distribution of the output beam is not gaussian or flat top in shape. The high intensity region of the beam is a crescent shaped

portion in the lower part of the mode (as determined by actual target damage regions). The performance of the laser is temperature sensitive. Between the two runs the atmospheric conditions could have changed sufficiently to cause a slightly different spatial intensity distribution yielding a different peak to average ratio and causing inconsistent results.

In a previous experiment at the Naval Postgraduate School, Beelby and Ulrich III discovered a similar inconsistency. They had done experimentation to determine the onset of arcing in a vacuum for various types of materials. It was determined that the onset of arcing for type 304 stainless steel was between 5.1 and 5.4 MW/cm^2. However, while determining the onset of arcing for aluminum 2024 a sample of this type of stainless steel was irradiated and no plasma or arcing was present at 10.9 MW/cm^2. [Ref.9]

In addition to the above explanations for the inconsistency in the data there are also measurement errors. The first, and possibly most significant, is the fact that in calculating power density for the onset of arcing, a uniform spatial intensity distribution is assumed. This is certainly not the case and in making this assumption large errors may result. Furthermore, the calculation also assumes that the temporal content of the beam is a step function, which is also not the case.

A second source of error results from measuring spot size. The spot size seen using the exposed Polaroid film has an average diameter on the order of .75cm. The response of the film to irradiation is not known exactly and the spot is slightly elliptical in shape. Assuming the measurement accuracy is 0.1 cm, a 3% error would result. Another assumption in calculating the power density was that each optical surface reflected 4% of the incident energy. The actual amount of reflected energy could not be measured. However, since the power meter was indirectly irradiated by the reflection from one of the optics, a slight error in the reflectivity could lead to relatively large measurement errors. Finally, the Energy Meter was calibrated to an accuracy of only 20%.

In lieu of these error sources, calculated power densities can only be assumed to be accurate to an order of magnitude.

c. Discussion of Results

Previous studies of unipolar arcing have been conducted at the Naval Postgraduate School. The equipment and experimental setup in these studies were, for the most part, identical to those used for this thesis. In particular, the laser (with its ancillary equipment), target chamber, optics, and power meter were identical. The

variable of concern in this experiment was ambient pressure. Previous work has involved placing the samples in the target chamber, evacuating the chamber and then irradiating the targets. For this experiment the target chamber was allowed to remain at atmospheric pressure. This section will discuss and compare results from previous work with that done for this thesis.

The damage mechanisms seen in this experiment were similar to those previously reported. Samples were observed to have evidence of melting and unipolar arcing. As the power density was decreased, unipolar arcing was the only damage mechanism present.

Samples irradiated at atmospheric pressure had the characteristic hemispherical shaped craters associated with unipolar arcing. The density of craters found at atmospheric pressure (1.7×10^6 craters per square centimeter) is an order of magnitude larger than previously reported values (3.0×10^5 craters per square centimeter) [Ref. 9]. There was also a difference found in the size of the crater rims. At atmospheric pressure the largest single craters found were approximately 13 microns in diameter while in a vacuum the longest burning arcs left craters up to 30-40 microns in diameter. The cathode spots were similar in size and nature.

The onset of arcing at atmospheric pressure for Aluminum 2024 was found to be between 6.8 and 20.3 MW/cm^2. In previous work done at the Naval Postgraduate School, Beelby and Ulrich III reported the onset of arcing for Aluminum 2024 in a vacuum to be between 4.6 and 11.2 MW/cm^2. Because of the accuracies of both of these measurements, the only conclusion which can be made is that the onset of arcing at atmospheric pressure occurs close to that of a target in a vacuum. That is, there does not appear to be a strong dependency on surrounding pressure.

B. ALUMINUM COATED GLASS SLIDES

1. Description

Numerous shots were made on the aluminum coated glass microscope slides. They were positioned outside of the target test chamber such that the incident beam made an angle of about 10 degrees relative to the surface normal. A narrow band filter (1.06μm) was placed immediately behind the coated slide and then a Polaroid camera was positioned to photograph the backside of the microscope slide. After the targets were irradiated, they were examined using an optical and scanning electron microscope (SEM).

Examining the damage using the SEM proved difficult due to the lack of conductivity of the surface of the target. (The SEM requires an electrically conductive surface in order

to function properly.) In the figures produced by the SEM, the horizontal light colored bands are a result of the poor conductivity.

2. Target Damage

After being irradiated, all of the targets had areas where the aluminum coating had been removed from the surface. The bright streaks in Figure 4.6 are the paths of molten aluminum particles occurring during the time the laser beam was incident on the target. The bright portion is indicative of a plasma being present. In Figure 4.7 a 90% attenuating broad band filter was placed before the camera. Again, the bright portion is evidence that a plasma was present and the crescent shape is where the aluminum was removed, corresponding to the high intensity portion of the beam. In the less intense regions of the beam the aluminum coating was not removed.

Within the high intensity region there were brown colored elliptical shaped areas of even higher intensity. Figure 4.8 shows a portion of the cresent shaped high damage region and Figures 4.9 and 4.10 show extremely high intensity regions. Figure 4.11 is a magnified view of Figure 4.10. From this it can be seen that there are small circular areas of damage (top central region and the region in the center of

Figure 4.6 Polaroid Photograph of Aluminum Covered Glass Slide

Figure 4.7 Same as above with a 90% Attenuating Filter

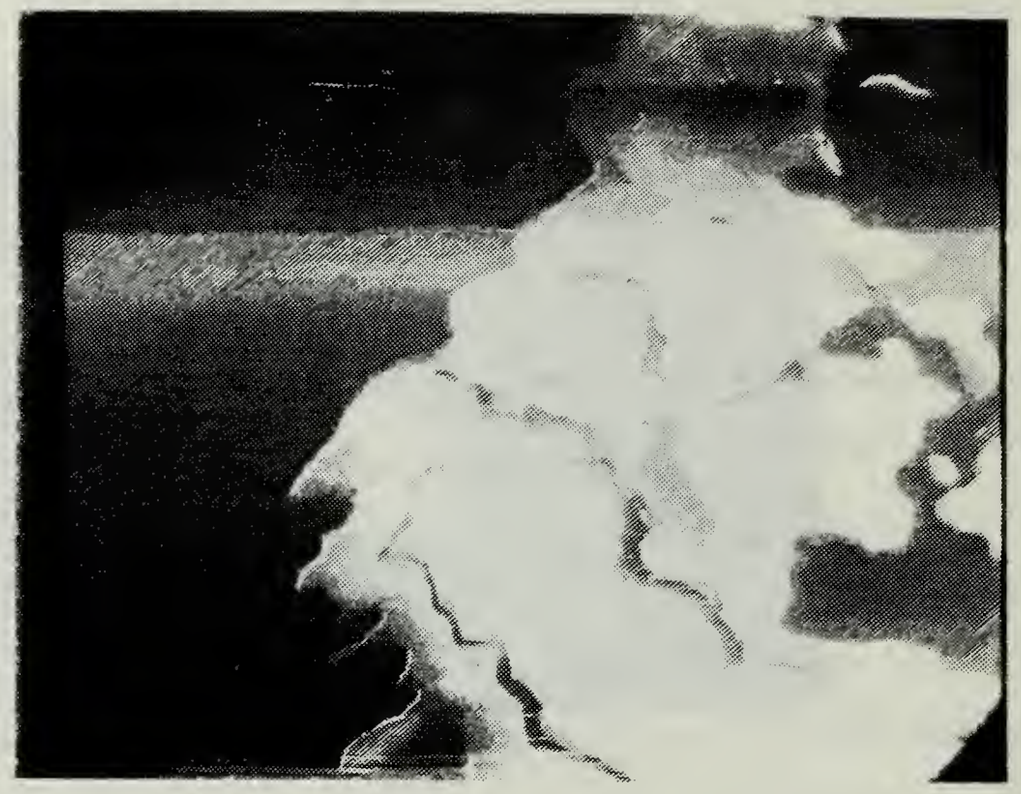

Figure 4.8 High Intensity Region of Aluminum Covered Glass Slide, 15X, SEM

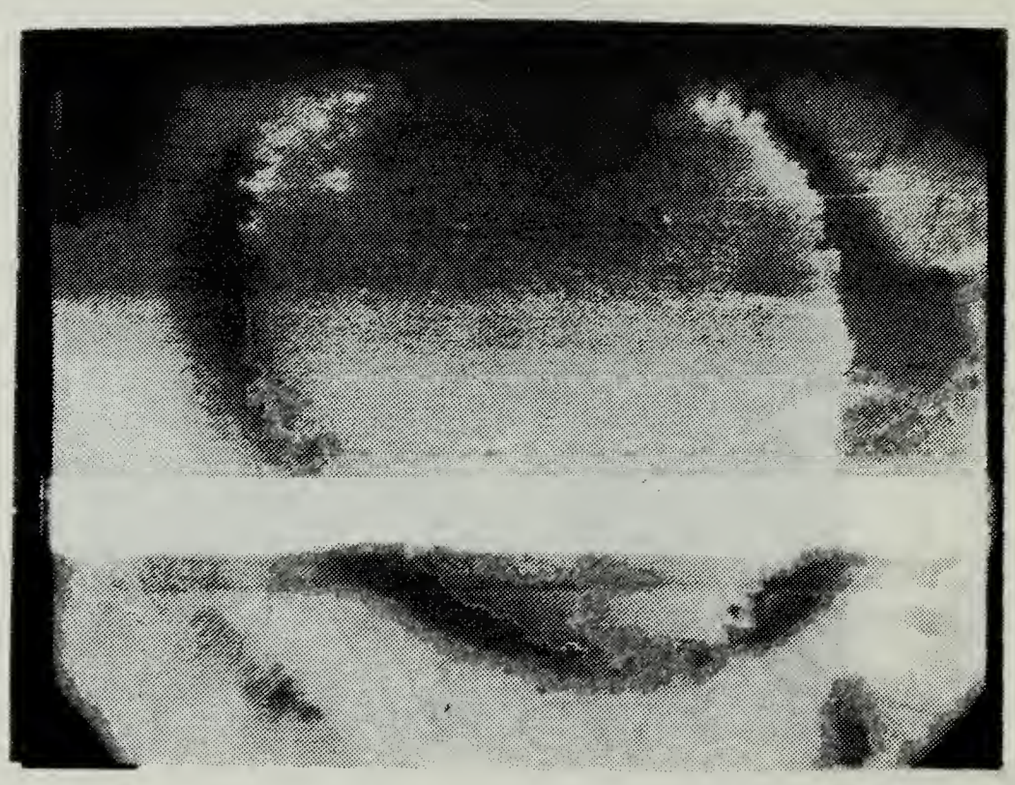

Figure 4.9 Hot Spot within High Intensity Region of Aluminum Covered Glass Slide, 75X, SEM

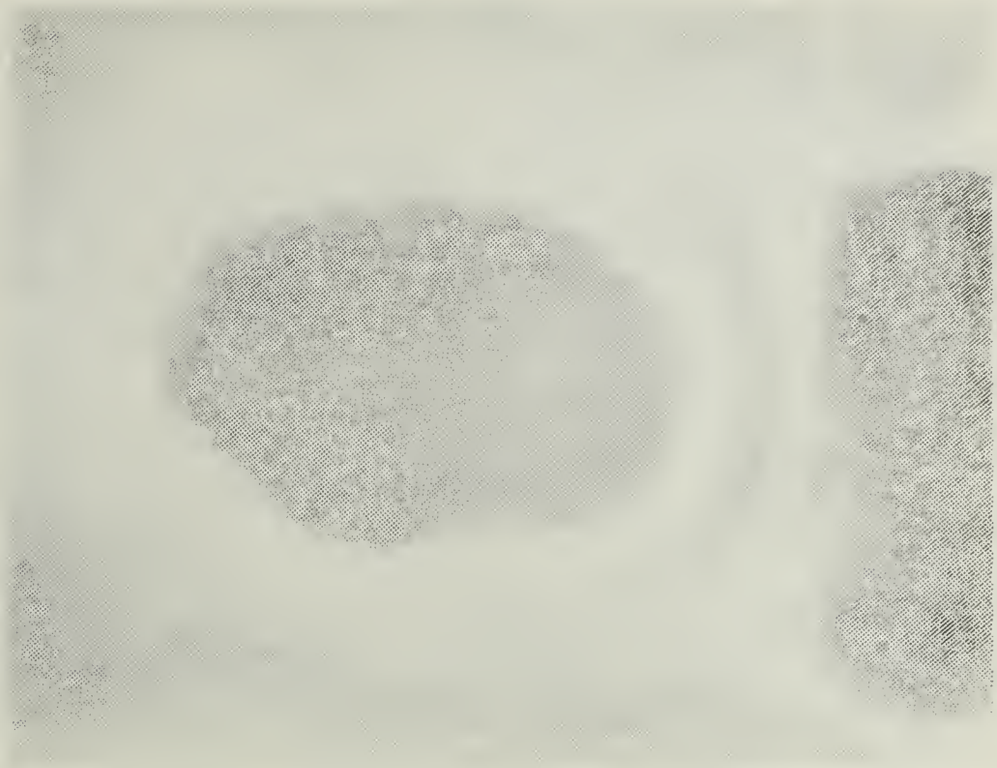

Figure 4.10 Hot Spot within High Intensity Region of Aluminum Covered Glass Slide, 50X Optical Microscope

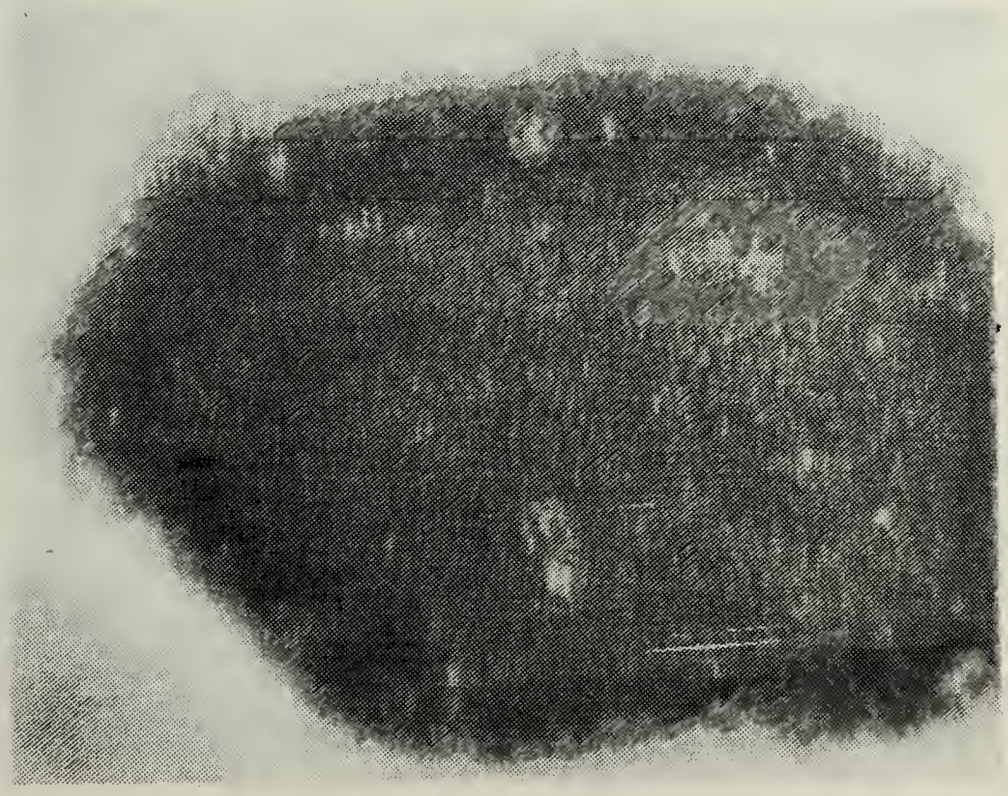

Figure 4.11 Hot Spot within High Intensity Region of Aluminum Covered Glass Slide, 100X, Optical Microscope

the photograph). Figure 4.12 is a magnified view of one of these regions. At 400X magnification on the optical microscope, Figure 4.13 shows that these areas are concentric rings. This interference pattern is seen frequently when studying unipolar arcing. The rings are a result of interference fringes from the laser and typically the high intensity bands have many unipolar arc craters while the low intensity regions have few or none. In this figure it is difficult to determine decisively if the unipolar arc craters are present, although in the central region where focus in the figure is the sharpest it appears that they are craterlike structures. The diameter of the crater is approximately 7.5 micrometers, corresponding to what would be expected if they were craters from unipolar arcing. Although clearly visible using an optical microscope, these regions did not appear using the scanning electron microscope.

A feature that was evident in the "hot spots" within the high intensity regions, using the scanning electron microscope, was barnacle appearing structures. The structures are shown in increasing magnification in Figures 4.14 through 4.16. The cores or "holes" in the center of the barnacles have diameters ranging from 0.3 to 1.9 microns, but are probably not unipolar arcs as they do not have the characteristic rims surrounding the cores. Similar structures have been observed previously with the conclusion

Figure 4.12 Magnified View of Figure 4.11, 200X, Optical Microscope

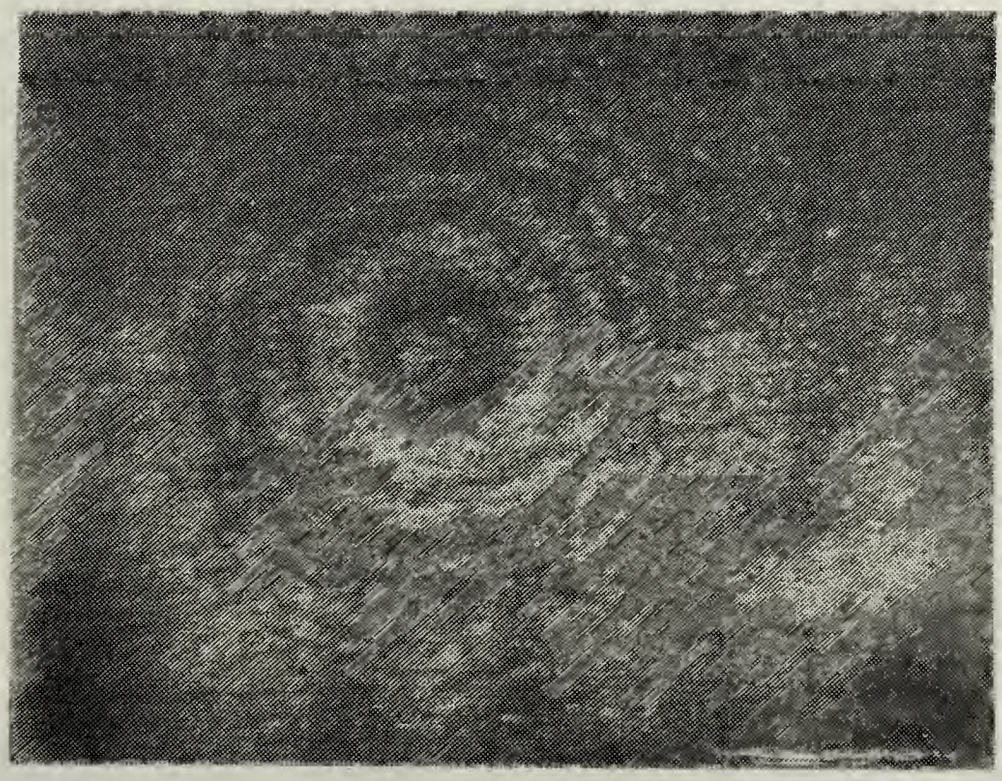

Figure 4.13 Concentric Rings Occurring in Hot Spots on Aluminum Coated Glass Slides, 400X, Optical Microscope

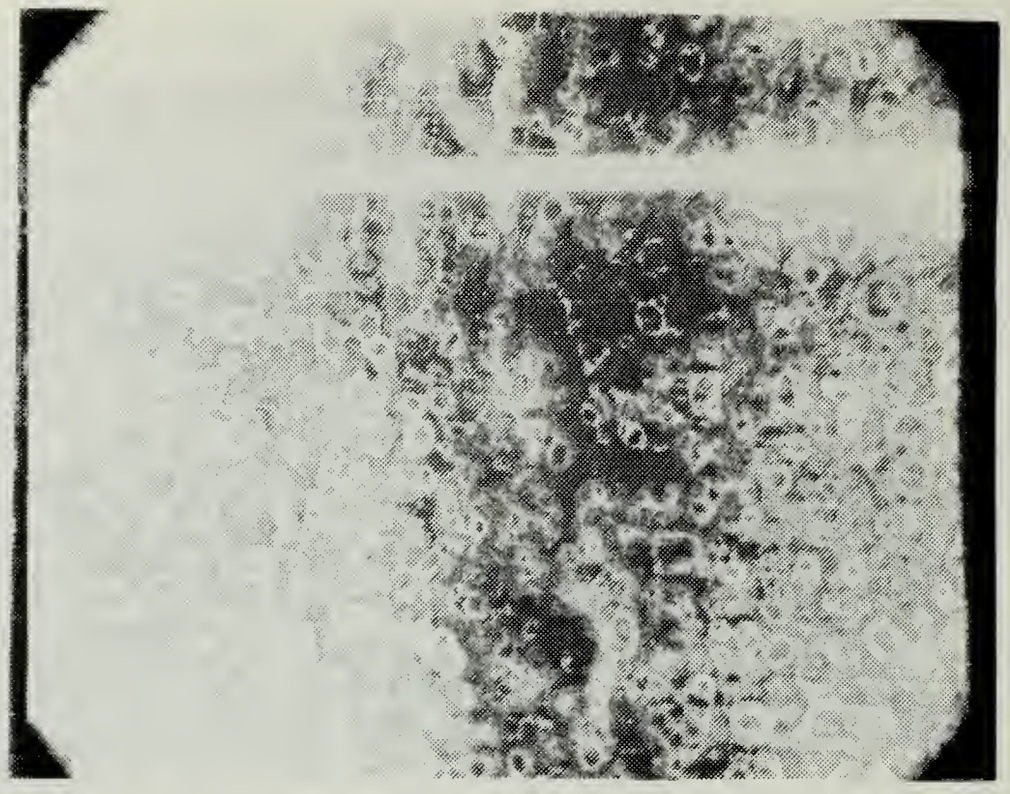

Figure 4.14 Barnacle-like Structures Appearing in Hot Spots, 760X, SEM

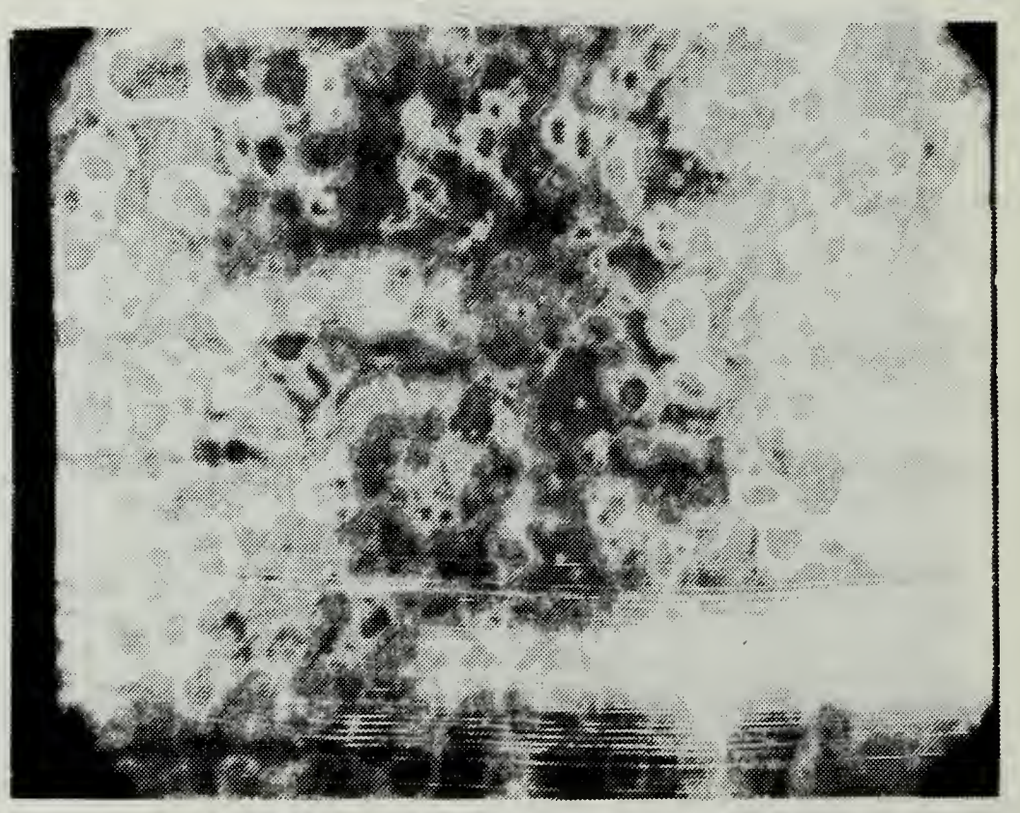

Figure 4.15 Same as above, 1500X, SEM

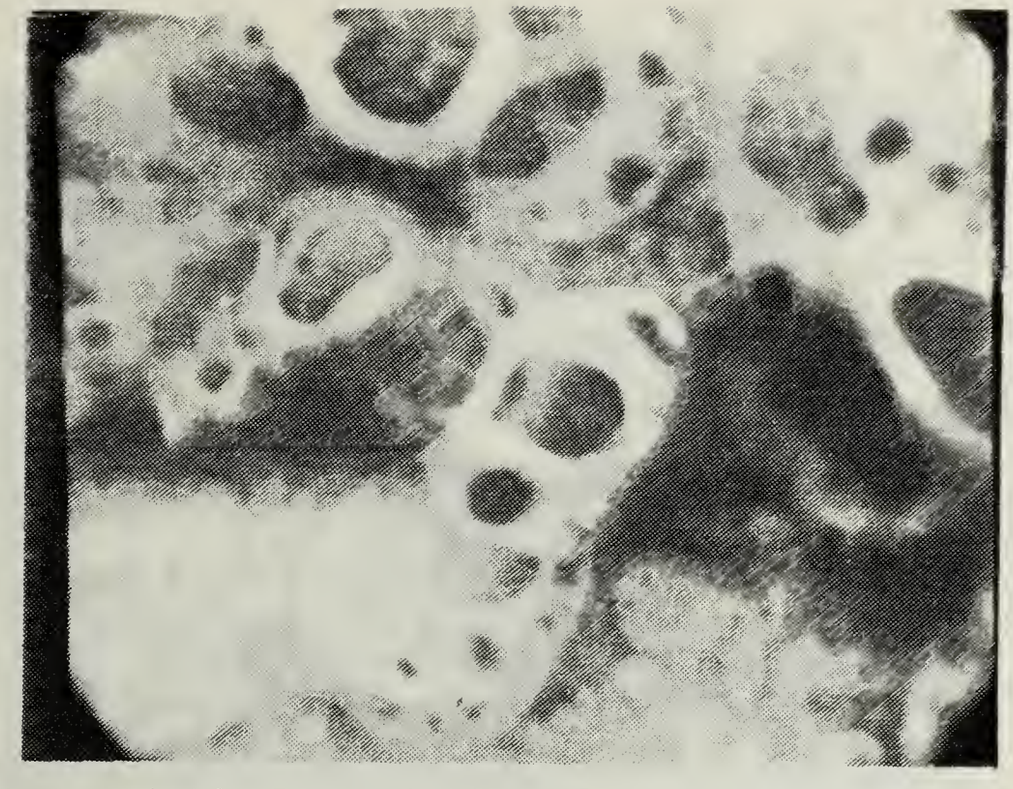

Figure 4.16 Barnacle-like Structures Appearing in Hot Spots, 7500X, SEM

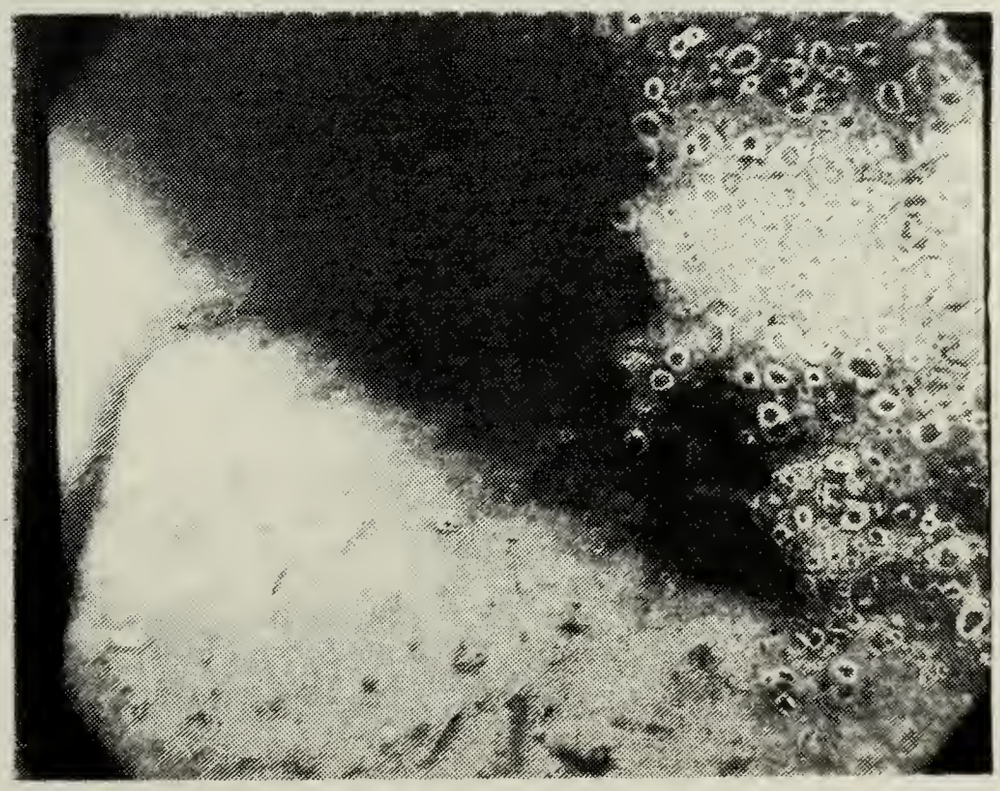

Figure 4.17 Boundary of Hot Spot Region, 760X, SEM

that since the samples were not outgassed, the barnacles may be a result of "expanding cavities" or "blisters" of trapped hydrogen due to the flash heating by the laser [Ref. 9]. Surface tension acting on the liquid metal can also contribute to the formation of the barnacle structures.

At the boundary of the "hot spots" the barnacles are no longer present and the surface becomes much smoother (see Figure 4.17). In this region there is no evidence of unipolar arcing.

In the lower intensity region, Figure 4.18 shows what appear to be craterlike formations. The diameters of these craters are .5 to 1.5 microns. These structures are likely to be unipolar arc craters with the rims not visible due to poor conductivity of the glass slide under the SEM.

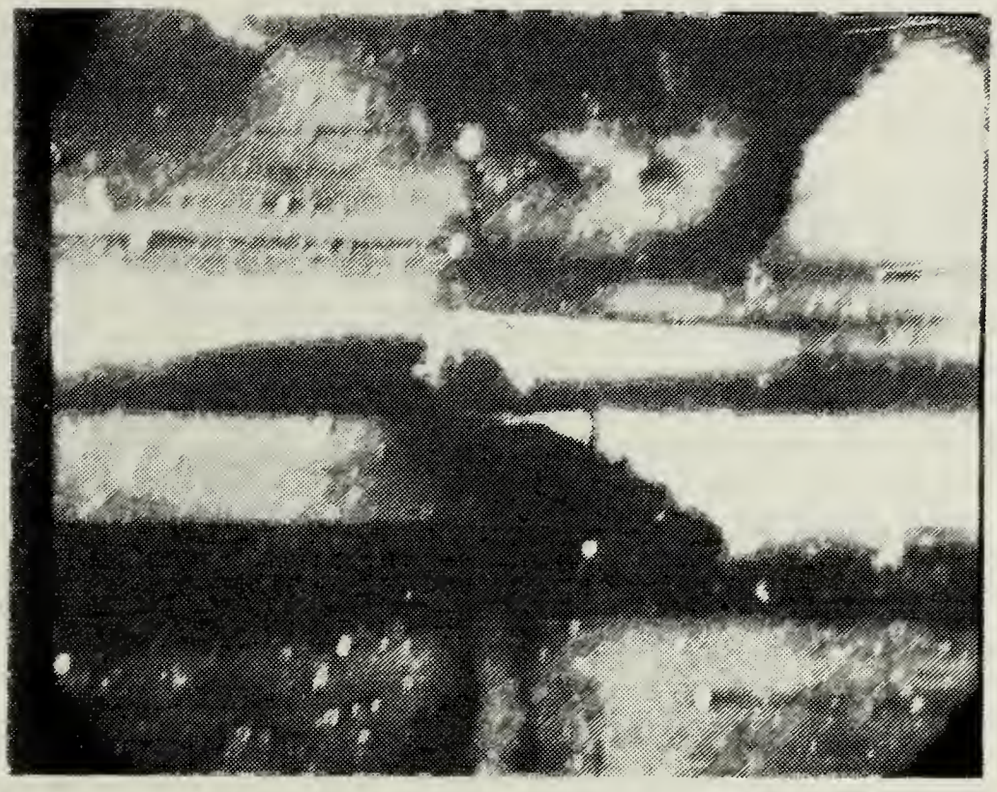

Figure 4.18 Craters in Low Intensity Region of Aluminum Covered Glass, 1500X, SEM

V. CONCLUSIONS

The study undertaken in this thesis examined the unipolar arcing phenomenon at atmospheric pressure. On the aluminum targets it was found that anytime there was a plasma present, unipolar arcing occurred. The power density required for the onset of arcing at atmospheric pressure was found to be similar to that in a vacuum, although the crater density was found to be an order of magnitude higher, while the size of the resulting craters was more than a factor of 2 smaller. This suggests that although the power density required to initiate arcing was similar at atmospheric pressure, more arc initiation sites are present. Consequently, in order to maintain a balance they burn less intensely.

The extremely high intensity regions on the aluminum coated glass slides when viewed under the SEM showed no evidence of unipolar arcing, but arc craters in these regions may have been obscured by the appearance of the barnacle-like structures. Using the optical microscope, these high intensity regions showed interference rings and craterlike structures which possibly were formed by unipolar arcing. In the regions of less intense radiation the barnacles were no longer seen and craters resembling those from unipolar arcing were apparent.

A previous study had suggested that the use of better vacuum systems would result in minimizing damage from unipolar arcing. This study suggests that while the number of arc sites may be minimized, the sites that did initiate and sustain an arc would burn more violently. The number of damaged spots from unipolar arcing would be fewer but the damage to the surface in these regions would be more drastic.

LIST OF REFERENCES

1. Behrisch, R., "Surface Erosion from Plasma Materials Interaction," Journal of Nuclear Materials, v. 85-86, p. 1047-1061, 1979.

2. Keville, M. T. and Lautrup, R. W., "An Investigation of Unipolar Arcing Damage on Stainless Steel and Titanium Carbide Coated Surfaces," M.S. Thesis, Naval Postgraduate School, Monterey, California, 1980.

3. Tazima, T., "First Wall Design Considerations of JT-60 and Related Experiments," Journal of Nuclear Materials, v. 76-77, p. 594-599, 1978.

4. Ryan, F. T. and Shedd, S. T., "A Study of the Unipolar Arcing Damage Mechanism on Selected Conductors and Semiconductors," M.S. Thesis, Naval Postgraduate School, Monterey, California, June 1981.

5. Goodall, D.H.J., Conlon, T. W., Sofield, C. and McCraken, G. M. "Investigations of Arcing in the DITE Tokamak," Journal of Nuclear Materials, v. 76-77, p. 492-498, 1978.

6. Schwirzke, F., "Basic Mechanisms that Lead to Laser Target Damage," Naval Postgraduate School Paper, Oct 1981.

7. Robson, A. E. and Thonemann, P. C., "An Arc Maintained on An Isolated Metal Plate Exposed to A Plasma," Institute of Electrical Engineers, v. 106, pt. A, supp. 2, p. 508-512, April 1959.

8. Chen, F., Introduction to Plasma Physics and Controlled Fusion, v. 1, Plenum Press, New York, N.Y., 1984.

9. Beelby, M. H. and Ulrich III, H. G., "A Study of the Breakdown Mechanism of AISI 304 Stainless Steel, Type 2024 Aluminum and Various Titanium Coatings," M.S. Thesis, Naval Postgraduate School, Monterey, California, 1981.

10. Schwirzke, F. and Taylor, R. J., "Surface Damage by Sheath Effects and Unipolar Arcs," Journal of Nuclear Materials, v. 93-94, p. 780-784, 1980.

11. Schwirzke, F., "Laser Induced Unipolar Arcing," Laser Interaction and Related Plasma Phenomena, v. 6, 1984.

12. Tien, J. K., Panayotou, N. F., Stevenson, R. D., and Gross, R. A., "Unipolar Arc Damage of Materials in a Hot, Dense Deuterium Plasma," Journal of Nuclear Materials, v. 76-77, p. 481-488, 1978.

INITIAL DISTRIBUTION LIST

		No. Copies
1.	Defense Technical Information Center Cameron Station Alexandria, Virginia 22304-6145	2
2.	Library, Code 0142 Naval Postgraduate School Monterey, California 93943-5002	2
3.	Professor K. E. Woehler, Code 61Wh Department of Physics Naval Postgraduate School Monterey, California 93943	1
4.	Professor F. Schwirzke, Code 61Sw Department of Physics Naval Postgraduate School Monterey, California 93943	2
5.	LT Steven W. Woodson, USN 202 Rossford White Sands Missile Range, New Mexico 88002	2

Thesis
W843757 Woodson
c.1 An investigation of unipolar arcing at atmospheric pressure in Aluminum 2024 and aluminum coated glass slides.